Cellular Biology

miR-146a Suppresses SUMO1 Expression and Induces Cardiac Dysfunction in Maladaptive Hypertrophy

Jae Gyun Oh, Shin Watanabe, Ahyoung Lee, Przemek A. Gorski, Philyoung Lee, Dongtak Jeong,
Lifan Liang, Yaxuan Liang, Alessia Baccarini, Susmita Sahoo, Brian D. Brown,
Roger J. Hajjar, Changwon Kho

Rationale: Abnormal SUMOylation has emerged as a characteristic of heart failure (HF) pathology. Previously, we found reduced SUMO1 (small ubiquitin-like modifier 1) expression and SERCA2a (sarcoplasmic reticulum Ca^{2+}-ATPase) SUMOylation in human and animal HF models. SUMO1 gene delivery or small molecule activation of SUMOylation restored SERCA2a SUMOylation and cardiac function in HF models. Despite the critical role of SUMO1 in HF, the regulatory mechanisms underlying SUMO1 expression are largely unknown.

Objective: To examine miR-146a–mediated SUMO1 regulation and its consequent effects on cardiac morphology and function.

Methods and Results: In this study, miR-146a was identified as a SUMO1-targeting microRNA in the heart. A strong correlation was observed between miR-146a and SUMO1 expression in failing mouse and human hearts. miR-146a was manipulated in cardiomyocytes through AAV9 (adeno-associated virus serotype 9)-mediated gene delivery, and cardiac morphology and function were analyzed by echocardiography and hemodynamics. Overexpression of miR-146a reduced SUMO1 expression, SERCA2a SUMOylation, and cardiac contractility in vitro and in vivo. The effects of miR-146a inhibition on HF pathophysiology were examined by transducing a tough decoy of miR-146a into mice subjected to transverse aortic constriction. miR-146a inhibition improved cardiac contractile function and normalized SUMO1 expression. The regulatory mechanisms of miR-146a upregulation were elucidated by examining the major miR-146a–producing cell types and transfer mechanisms. Notably, transdifferentiation of fibroblasts triggered miR-146a overexpression and secretion through extracellular vesicles, and the extracellular vesicle–associated miR-146a transfer was identified as the causative mechanism of miR-146a upregulation in failing cardiomyocytes. Finally, extracellular vesicles isolated from failing hearts were shown to contain high levels of miR-146a and exerted negative effects on the SUMO1/SERCA2a signaling axis and hence cardiomyocyte contractility.

Conclusions: Taken together, our results show that miR-146a is a novel regulator of the SUMOylation machinery in the heart, which can be targeted for therapeutic intervention. (*Circ Res*. 2018;123:673-685. DOI: 10.1161/CIRCRESAHA.118.312751.)

Key Words: extracellular vesicle ■ heart failure ■ mice ■ microRNA ■ sarcoplasmic reticulum

Ca^{2+} cycling abnormalities in cardiomyocytes have been shown to be critical in the pathophysiology of heart failure (HF).[1–3] Experimental studies have demonstrated that stabilization of Ca^{2+} cycling significantly rescues the HF phenotype and increases animal survival. In this regard, the SERCA2a (sarcoplasmic reticulum Ca^{2+}-ATPase) pump and its regulators have been shown to be important targets for intervention.[4–9] Previously, our group identified SUMO1 (small ubiquitin-like modifier 1) as a positive regulator of SERCA2a that exhibits reduced levels during HF.[10] SERCA2a undergoes SUMOylation at lysine sites 480 and 585 by SUMO1,

rendering it more stable and increasing its activity.[10] Gene transfer of SUMO1 normalizes SUMO1 expression, enhances SERCA2a SUMOylation, and restores cardiac function in both mouse and swine HF models.[10–12] However, the regulatory mechanisms underlying the downregulation of SUMO1 expression have yet to be elucidated.

MicroRNAs (miRs) are short single-stranded noncoding RNAs that evolved to fine-tune biological networks by destabilization and translational inhibition of target mRNAs.[13] Alterations in the levels of several miRs (ie, miR-1, -21, and

Novelty and Significance

What Is Known?

- SUMO1 (small ubiquitin-like modifier 1) regulates the SERCA2a (sarcoplasmic reticulum Ca^{2+}-ATPase) pump and has emerged as a validated molecular target for heart failure.
- SUMO1 and SUMOylated SERCA2a levels are reduced in failing hearts and enhancing SUMO1 by gene delivery or pharmacological activation rescues the heart failure phenotype in animal models.
- The regulatory mechanisms underlying SUMO1 expression in the heart are unknown.

What New Information Does This Article Contribute?

- MicroRNA-146a regulates SUMO1/SERCA2a axis in cardiomyocytes, and its upregulation contributes to the contractile dysfunction in heart failure.

- Mir-146a is secreted from transdifferentiated fibroblasts and then transferred into cardiomyocytes through extracellular vehicles–mediated trafficking and inhibits the SUMO1 expression.
- Inhibition of miR-146a reverses contractile dysfunction by restoring SUMO1 levels in mice with pathological cardiac hypertrophy.

SUMO1 is identified, as a new therapeutic target molecule for heart failure; however, its regulatory mechanism has not been explored. For the first time, we report that miR-146a induction plays a critical role in the abnormal regulation of SUMO1 pathway. In addition, we validated the delivery of miR-146a from cardiac fibroblasts into cardiomyocytes through extracellular vehicles. The beneficial effects of miR-146a inhibition on cardiac function suggest that targeting miR-146a may provide a novel therapeutic strategy for the treatment of heart failure.

Nonstandard Abbreviations and Acronyms

AAV9	adeno-associated virus serotype 9
DLST	dihydrolipoyl succinyltransferase
ERBB4	Erb-B2 receptor tyrosine kinase 4
EV	extracellular vesicle
Fib-EV	EVs isolated from fibroblast cultures
HF	heart failure
IRAK1	interleukin-1 receptor-associated kinase 1
NRAS	neuroblastoma RAS viral oncogene homolog
qRT-PCR	quantitative reverse transcription polymerase chain reaction
SERCA2a	sarcoplasmic reticulum Ca^{2+}-ATPase
SUMO1	small ubiquitin-like modifier 1
TAC	transverse aortic constriction
TGF-β	transforming growth factor-β
TNF	tumor necrosis factor
TRAF6	TNF receptor–associated factor 6
UTR	untranslated region

-133) have been observed in human failing myocardium.[14] Single miR tends to regulate multiple targets within the same functional pathway. Furthermore, miR-targeting drugs are unlikely to be limited by immunologic issues that commonly accompany virus-mediated gene therapy.[15] Therefore, miRs are attractive targets for human diseases including HF. For example, our group found that miR-25 downregulates SERCA2a expression and that miR-25 inhibition enhances Ca^{2+} handling and cardiac function through the restoration of SERCA2a levels in failing mouse hearts.[16] In the present study, we discovered that miR-146a negatively regulates Ca^{2+} cycling by downregulating SUMO1 expression.

miR-146a was initially reported to act as a negative regulator of innate immune responses by targeting IRAK1 (interleukin-1 receptor-associated kinase 1) and TRAF6 (tumor necrosis factor receptor–associated factor 6).[17] Thus, downregulation of miR-146a is closely associated with autoimmune diseases.[18–20] The role of miR-146a in the heart has been shown to vary by heart disease model. Overexpression of miR-146a has exerted beneficial effects by suppressing excessive immune responses in ischemia/reperfusion injury,[21] septic cardiomyopathy,[22] and diabetic cardiomyopathy models.[23] In contrast, miR-146a overexpression has shown to have deleterious effects such as reduced cardiac function and adverse cardiac remodeling in doxorubicin-induced cardiomyopathy,[24] peripartum cardiomyopathy,[25] and pressure overload models[26] by targeting genes such as *Erbb4*, *Nras*, or *Dlst*. Therefore, the conclusive role of miR-146a during HF has yet to be defined.

Here, we tested the effects of miR-146a modulation in transverse aortic constriction (TAC)–induced HF models and validated the role of miR-146a as a SUMO1-targeting miR. We discovered that miR-146a expression correlates inversely with SUMO1 expression in failing human and mouse hearts. Using genetic techniques, we demonstrated that overexpression of miR-146a attenuates SUMO1 expression, SERCA2a SUMOylation, and cardiac contractile function in vitro and in vivo. In contrast, inhibition of miR-146a normalizes these alternations by the elevated miR-146a levels in the failing conditions. Furthermore, we found that miR-146a is formed in fibroblasts, but not in cardiomyocytes, and then released as an extracellular vesicle (EV)–associated form. The EV-associated miR-146a is transferred into cardiomyocytes and attenuates SUMO1 expression, thereby reducing contractile function. Collectively, we demonstrate a novel mechanism underlying the regulation of SUMO1 expression, which provides novel insights into cardiac intercellular communication in HF.

Methods

All in vivo cardiac function data have been made publicly available at figshare and can be accessed at 10.6084/m9.figshare.6932888 or from the corresponding author on request. Detailed Methods section is available in the Online Data Supplement.

EV Treatment

Our fluorescence-activated cell sorting and nanoparticle tracking analysis revealed the number of cardiac cells and EVs from normal and failing hearts to have the ratio of 1:2000 (cells:EVs). Thus, the EVs were treated at the rate of 2000 in EV treatment experiments. The isolated adult cardiomyocytes were treated with purified EVs for 24 hours after which RNA and contractile properties of cardiomyocytes were analyzed.

EV Labeling and Confocal Analysis

EVs were subjected to PKH26 labeling according to the manufacturer's recommendations. For confocal laser scanning microscopy experiments, cardiomyocytes were incubated with PKH26-labeled EVs (2000 EVs per cell) for 24 hours. Cardiomyocytes were washed twice with PBS solution to remove surface-associated EVs and were then fixed in 2% (wt/vol) paraformaldehyde for 5 minutes on ice. Cardiomyocytes were imaged using Leica SP5 CLSM confocal microscope.

Statistical Analysis

Data are expressed as mean±SEM as indicated. All data were analyzed using the Student *t* test for comparison of 2 groups and 1-way ANOVA for 3 groups. Survival testing was performed with the Kaplan-Meier analysis. To assess the correlation between miR-146a expression and SUMO1 expression, we used Spearman correlation and plotted individual relative expressions of miR-146a and SUMO1 that were normalized by 18S RNA expression. For all in vivo experiments, the groups were randomly allocated and examined under blind test conditions. Statistical outliers were not automatically excluded; only technical failures or sudden death were excluded from the data sets. Differences were considered statistically significant when the *P* value was <0.05.

Results

miR-146a Directly Targets SUMO1 in Cardiomyocytes

To gain a better understanding of the regulatory mechanisms underlying decreased SUMO1 expression during HF, we sought to identify miRs that affect the expression of SUMO1 using in silico screening methods. Four different prediction programs (microRNA.org, miRSearch, DIANA, and mirdb.org) all yielded miR-146a as a strong candidate (Online Figure IA). The *Sumo1* 3′-untranslated region (UTR) contains a putative miR-146a binding site that is highly conserved among selected vertebrates (Online Figure IB). Intriguingly, miR-146a was previously shown to affect Ca^{2+} handling in cardiomyocytes.[16] Quantitative reverse transcription polymerase chain reaction (qRT-PCR) analyses revealed that miR-146a levels were significantly elevated in failing human and mouse hearts (Figure 1A and 1B) and that miR-146a and SUMO1 levels were inversely
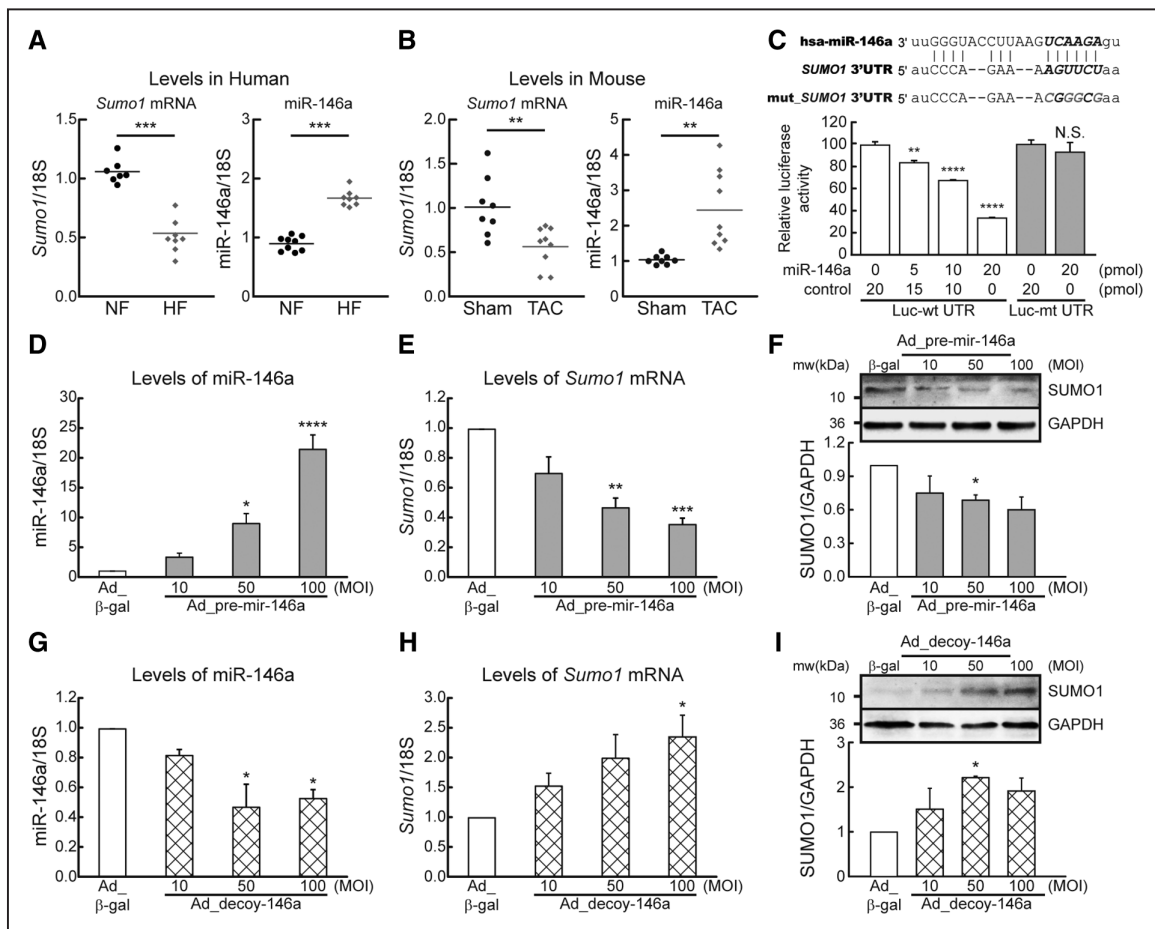
Figure 1. MicroRNA-146a (miR-146a) inhibits SUMO1 (small ubiquitin-like modifier 1) expression in cardiomyocytes. A, Changes in SUMO1 mRNA and miR-146a levels in human hearts of nonfailing (NF) and heart failure (HF) patients (n=7–9). **B**, Changes in SUMO1 mRNA and miR-146a levels in mouse hearts of sham-operated and transverse aortic constriction (TAC)–operated mice (6 wk after TAC) (n=8–9). **C**, Sequence alignment of SUMO1 wild-type and mutant 3′ untranslated regions (UTRs) with miR-146a (**top**) and luciferase reporter assay (**bottom**). Luciferase reporters with a putative miR-146a binding site (Luc-wt UTR [wild-type Sumo1 3'-UTR contained with the miR-146a binding site]) or mutant miR-146a–binding site (Luc-mt UTR [mutated Sumo1 3'-UTR]) were cotransfected into H9C2 cells with miR-146a mimic or control (cel-miR-39 [Caenorhabditis elegans miR-39]) for 24 h, and luciferase activity determined. Values are presented as relative luciferase activity±SEM (n=3). **D, E**, The expression of miR-146a (**D**) and SUMO1 mRNA (**E**) in isolated adult mouse cardiomyocytes which were infected with an adenovirus encoding pre-mir-146a (Ad_pre-mir-146a) for 48 h (n=3). **F**, Representative blot (**top**) and quantitative analysis (**bottom**) showing the expression of SUMO1 protein. **G, H**, The expression of miR-146a (**G**) and SUMO1 mRNA (**H**) in isolated adult mouse cardiomyocytes which were infected with an adenovirus encoding mir-146a decoy (Ad_decoy-146a) for 48 h (n=3). **I**, Representative blot (**top**) and quantitative analysis (**bottom**) showing the expression of SUMO1 protein. *P<0.05, **P<0.01, ***P<0.001, ****P<0.0001 vs the respective control, as determined by 1-way ANOVA. Data are presented as mean±SEM. MOI indicates multiplicity of infection; and N.S., not significant.

correlated in these hearts (Online Figure ID and IE). miR-146b shares a seed sequence with miR-146a[27]; however, its expression was not altered in failing hearts (Online Figure IC). Thus, in this study, we focused predominantly on examining the role of miR-146a. A luciferase reporter assay was used to test whether miR-146a binds directly to the *Sumo1* 3′-UTR. A miR-146a mimic suppressed the luciferase activity of a reporter containing the *Sumo1* mRNA 3′-UTR sequence in a dose-dependent manner (Figure 1C). This suppressive effect was abolished when the putative miR-146a binding site was mutated in the *Sumo1* 3′-UTR sequence (Figure 1C), indicating that miR-146a binding is specific. Isolated adult mouse cardiomyocytes treated with an adenovirus encoding pre-mir-146a (Ad_pre-mir-146a) exhibited a significant dose-dependent reduction in SUMO1 and SUMO1 conjugate levels, as assessed by qRT-PCR and Western blotting (Figure 1D through 1F and Online Figure IF). In striking contrast, treatment with an adenovirus encoding a tough decoy[28] for miR-146a (Ad_decoy-146a) led to a significant dose-dependent elevation in SUMO1 and SUMO1 conjugate levels (Figure 1G through 1I and Online Figure IG). Taken together, these data suggest that miR-146a regulates SUMO1 expression through specific binding to the 3′-UTR of SUMO1.

miR-146a Regulates Ca²⁺ Cycling in Cardiomyocytes

Reduced SUMO1 levels result in decreased SUMOylation of SERCA2a, which in turn leads to abnormal Ca^{2+} handling in failing hearts.[10] Therefore, we next examined the effect of miR-146a overexpression on SERCA2a SUMOylation and Ca^{2+} handling in cardiomyocytes. Ad_pre-mir-146a reduced SERCA2a SUMOylation by 30% in cardiomyocytes (Figure 2A). The expression levels of SUMO2, SUMO3, and other SUMOylation-related enzymes were not affected by miR-146a (Online Figure IIA through IIG). Moreover, Ad_pre-mir-146a reduced cardiomyocyte Ca^{2+} transient amplitude, SR Ca^{2+} load, and peak shortening and prolonged the time constant for Ca^{2+} transient decay (τ) as assessed by a dual-excitation fluorescent photomultiplier system (Figure 2B through 2F and Online Table I). The effects of miR-146a inhibition were examined in failing cardiomyocytes (Online Figure IIH). Inhibition of miR-146a by Ad_decoy-146a restored SUMO1 expression and SERCA2a SUMOylation (Figure 2G, Online Figure III and IIJ) and improved Ca^{2+} transient and contractility in failing cardiomyocytes (Figure 2H through 2L and Online Table I). In summary, these data suggest that miR-146a causes abnormal Ca^{2+} handling in cardiomyocytes through the suppression of SUMO1 expression and the inhibition of miR-146a significantly improves Ca^{2+} handling in failing cardiomyocytes in vitro.

Overexpression of miR-146a Impairs Cardiac Function In Vivo

These findings led us to investigate the in vivo role of miR-146a in HF. To characterize the physiological consequences of miR-146a overexpression, adeno-associated virus serotype 9 encoding pre-mir-146a (rAAV9_pre-mir-146a) or rAAV9-LacZ (beta-galactosidase; control) was administered to wild-type mice via the tail vein, and cardiac morphology and function were monitored at 4 weeks post gene delivery (Figure 3A). miR-146a levels were significantly increased in cardiomyocytes after injection of rAAV9_pre-mir-146a in a dose-dependent manner (Figure 3B and Online Figure IIIA through IIIC). Hypertrophic indices including heart weight/body weight ratio, left ventricle wall thickness, the left ventricle cardiomyocyte size, and hypertrophic marker expressions (ANF [atrial natriuretic factor], BNP [brain natriuretic peptide]) increased at 4 weeks postinjection of rAAV9_pre-mir-146a, compared with mice injected with the control virus (Figure 3C and 3D, Online Figure IIIF and IIIG and Online Table II). Mice with overexpressed miR-146a also exhibited a significant reduction in ventricular systolic function, as evidenced by the dose-dependent reduction in fractional shortening (FS) and ejection fraction (Figure 3D and 3E, Online Figure IIID and IIIE, and Online Table II). Moreover, hemodynamic analyses also revealed that left ventricle systolic function was significantly decreased in mice injected with rAAV9-pre-mir-146a, as indicated by the reduced end-systolic pressure-volume relationship and the maximum rate of pressure change (Max dP/dt) (Figure 3F and 3G and Online Table III). These data suggest that miR-146a overexpression resulted in cardiac systolic dysfunction. Furthermore, the rightward shift of pressure-volume loops observed in mice with overexpressed miR-146a indicated that miR-146a induced ventricular dilation (Figure 3F). SUMO1 expression was significantly decreased in mice injected with rAAV9_pre-mir-146a. SERCA2a expression and SUMOylation levels were also significantly reduced (Figure 3H through 3K, Online Figure IIIH and IIII). Overall, these data suggest that elevated miR-146a levels lead to dysregulation of the SUMO1/SERCA2a signaling axis and concomitant deterioration of cardiac morphology and function.

Inhibition of miR-146a Is Cardioprotective In Vivo

To evaluate the consequences of miR-146a inhibition, we examined the cardiac function of wild-type and TAC mice injected with either decoy-146a (rAAV9_decoy-146a) or rAAV9-LacZ (control). Wild-type mice were subjected to TAC surgery to induce pressure overload. The rAAV9_decoy-146a or control virus was injected at 2 weeks post-TAC, and cardiac morphology and function were monitored biweekly (Figure 4A). miR-146a levels were elevated in hearts injected with the control virus at 6 weeks post-TAC; however, miR-146a levels were completely normalized in hearts injected with the rAAV9_decoy-146a (Figure 4B and Online Figure IVA). Various hypertrophic markers were prominently increased in TAC mice injected with the control virus. In contrast, the hypertrophic response was blunted in TAC mice injected with the rAAV9_decoy-146a (Figure 4C and 4D, Online Figure IVC through IVE and Table IX). Adverse cardiac remodeling and functional deterioration were evident in mice treated with the control virus under pressure overload, but significantly attenuated in mice injected with the rAAV9_decoy-146a, as determined by FS and ejection fraction (Figure 4D and 4E, Online Figure IVB and Online Table IV). Hemodynamic analyses revealed that the left ventricle systolic function index (end-systolic pressure-volume relationship and Max dP/dt) was restored to normal levels, and ventricular dilation was
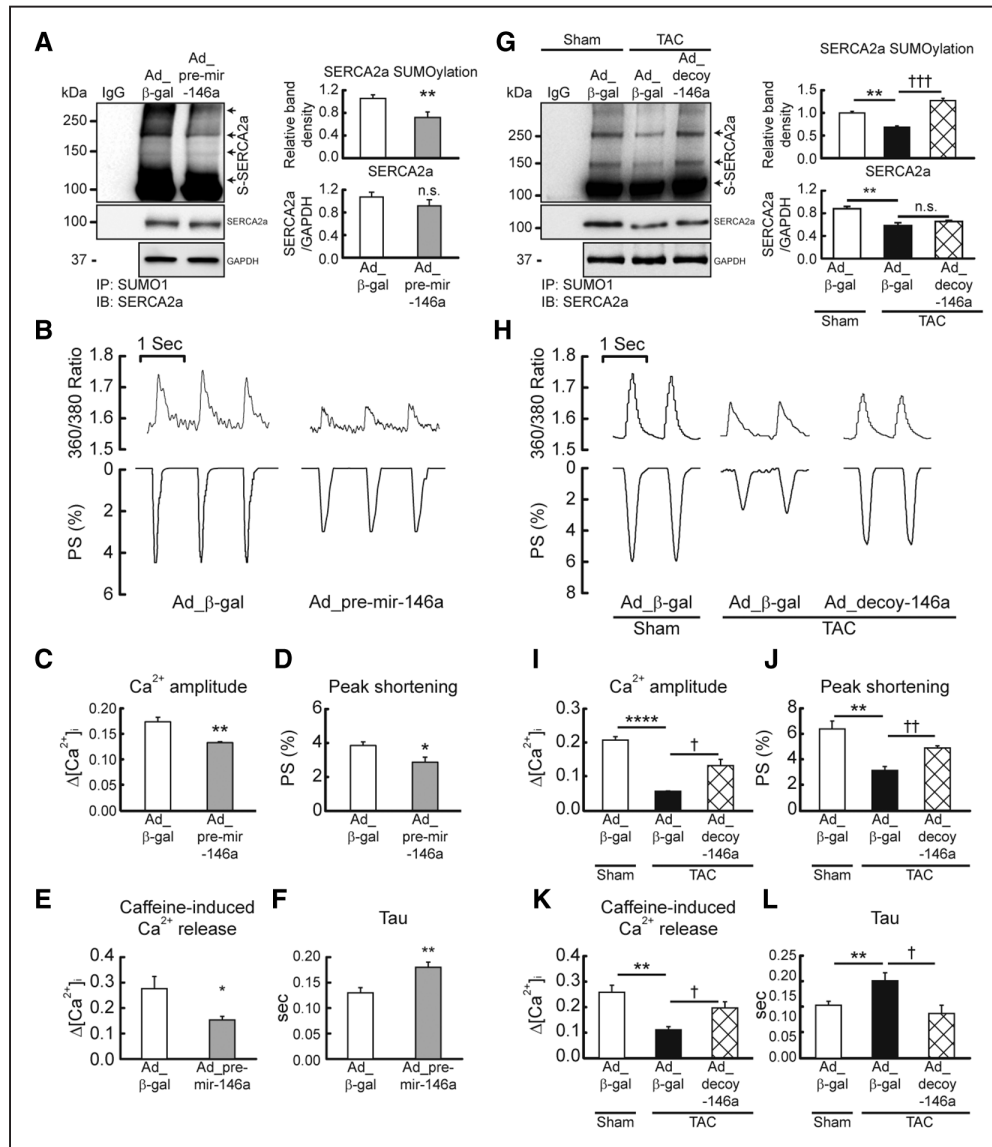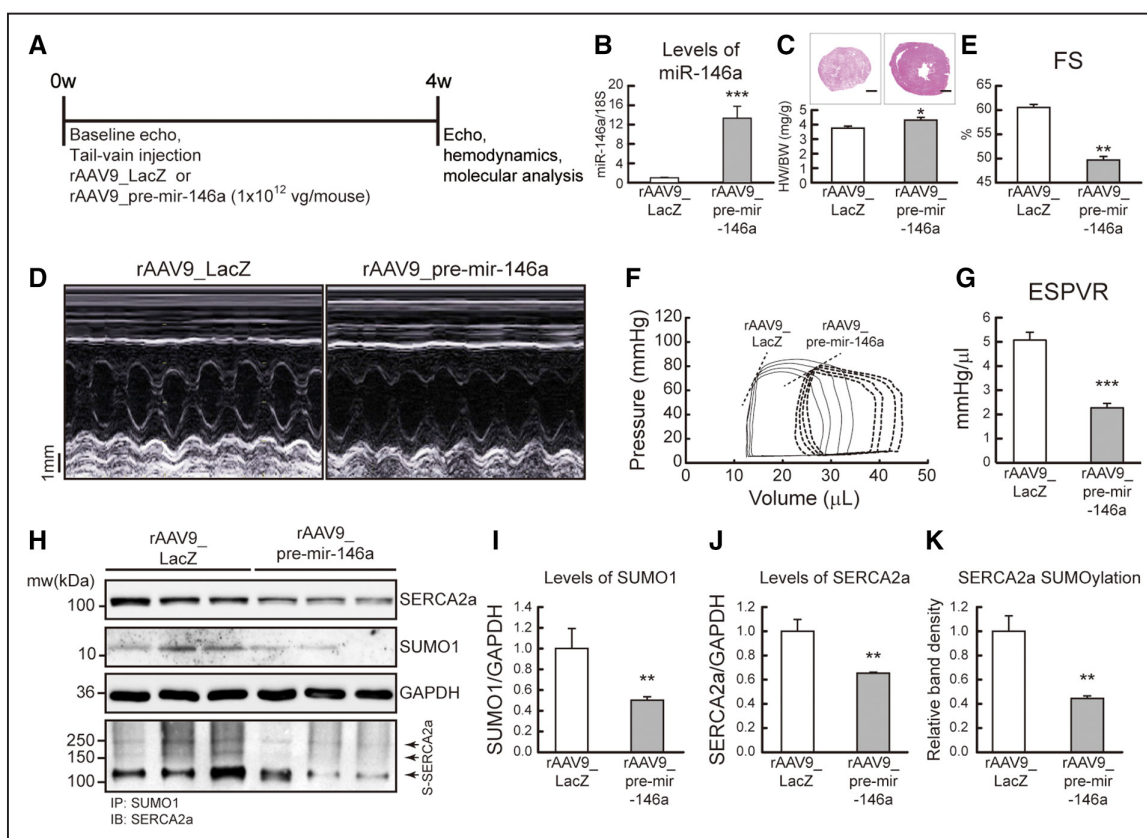
Figure 2. MicroRNA-146a (miR-146a) inhibits cardiac contractility via suppression of SERCA2a (sarcoplasmic reticulum Ca²⁺-ATPase) SUMOylation. Isolated mouse cardiomyocytes infected with Ad_pre-mir-146a (multiplicity of infection [MOI]=50) for 48 h. **A**, Representative blot (**left**) and quantitative analysis (**right**) showing the levels of SERCA2a SUMOylation and SERCA2a expression (n=6). **B**, Representative trace of calcium transients (**top**) and cardiac contractility (**bottom**). **C, D**, Averaged data of calcium transient amplitude (**C**) and sarcomere length shortening (**D**) (n=100–150 cells per 4 hearts). **E**, Caffeine-induced Ca²⁺ transient amplitude at 10 mmol/L Caffeine (n=10 cells/3 hearts). **F**, Rate constant for the decay of the Ca²⁺ transient (n=100–150 cells per 4 hearts). *$P<0.05$, **$P<0.01$ vs cardiomyocytes infected with Ad_β-gal, as determined by Student t test. Isolated failing cardiomyocytes from mice subjected to transverse aortic constriction (TAC) for 6 wk infected with Ad_decoy-146a (MOI=50) for 48 h. **G**, Representative blot (**left**) and quantitative analysis (**right**) showing the levels of SERCA2a SUMOylation and SERCA2a expression (n=3). **H**, Representative trace of calcium transients (**top**) and cardiac contractility (**bottom**). **I, J**, Averaged data of calcium transient amplitude (**I**) and sarcomere length shortening (**J**) (n=100–150 cells per 4 hearts). **K**, Caffeine-induced Ca²⁺ transient amplitude at 10 mmol/L Caffeine (n=10 cells per 3 hearts). **L**, Rate constant for the decay of the Ca²⁺ transient (n=100–150 cells per 4 hearts). *$P<0.05$, **$P<0.01$, ****$P<0.0001$ vs the sham mouse and †$P<0.05$, ††$P<0.01$ vs the failing cardiomyocyte treated with Ad_β-gal, as determined by 1-way ANOVA. Data are represented as mean±SEM. IB indicates immunoblotting; IP, immunoprecipitation; N.S., not significant; and PS, peak shortening.

normalized in TAC mice injected with the rAAV9_decoy-146a (Figure 4F and 4G and Online Table V). Western blotting showed that SUMO1, SUMO1 conjugates, SERCA2a, and SERCA2a SUMOylation levels were reduced under pressure overload, but were all normalized by rAAV9_decoy-146a under the same conditions (Figure 4H through 4K and Online Figure IVF through IVK). Taken together, these results demonstrate that inhibition of miR-146a improves cardiac function through the restoration of SUMO1 expression, which could potentially serve as a therapeutic target for HF.

Normalization of SUMO1 Levels Alleviates miR-146a–Mediated Cardiac Dysfunction

To confirm our hypothesis that elevated levels of miR-146a induce cardiac dysfunction by downregulating SUMO1, we used the strategy of restoring SUMO1 expression in a miR-146a overexpression model. Cardiac-specific Cre/loxP-conditional *Sumo1*-transgenic mice (SUMO1 TG) and their negative littermates were injected with rAAV9_pre-mir-146a, and tamoxifen was administrated at 2 weeks postviral injection to induce SUMO1 transgene expression. Cardiac function was analyzed at

Figure 3. Overexpression of microRNA-146a (miR-146a) promotes cardiac dysfunction in vivo. A, Protocol for AAV9 (adeno-associated virus serotype 9)-mediated pre-mir-146a gene transfer into normal mice. Six-week-old male B6C3/F1 mice received AAV9 carrying pre-mir-146a (rAAV9_pre-mir-146a, 1×10^{12} vg per mouse) or control virus (rAAV9_LacZ [beta-galactosidase]) via tail vein injection. After 4 wk of gene delivery, cardiac function was measured by echocardiography and then further analyzed by hemodynamic measurements. **B**, Levels of miR-146a. **C**, Cross-section images of a mouse heart **(top)** and quantification of heart weight/body weight ratio **(bottom)**. Scale bars, 1 mm. **D**, **E**, Representative left ventricle (LV) M-mode images **(D)** and factional shortening (FS) **(E)** (n=8). **F**, **G**, Representative pressure-volume loops **(F)** and end-systolic pressure-volume relationship (ESPVR; **G**) (n=6). **G**, Representative blot showing SERCA2a (sarcoplasmic reticulum Ca²⁺-ATPase), SUMO1 (small ubiquitin-like modifier 1), and total SUMOylation levels after infection with rAAV9_pre-mir-146a. **I–K**, The protein quantification of SUMO1 **(I)**, SERCA2a **(J)**, and SERCA2a SUMOylation **(K)** (n=6). *$P<0.05$, **$P<0.01$, ***$P<0.001$ vs mouse infected with rAAV9_LacZ, as determined by Student t test. Data are presented as mean±SEM. EV indicates extracellular vesicle; Fib-EV, EVs isolated from fibroblast cultures; TAC, transverse aortic constriction; and TGF-β, transforming growth factor-β.

6 weeks posttamoxifen administration (Figure 5A). Consistent with the data shown in Figures 3 and 4, SUMO1 levels were significantly reduced in negative littermates mice, but remained at near-normal levels in SUMO1 TG mice under conditions of miR-146a overexpression (Figure 5B and 5C, Online Figure VA and VC). The SUMOylation assay revealed that reduced SERCA2a SUMOylation under miR-146a overexpression was normalized in SUMO1 TG mice (Figure 5B and 5D). Normalization of SUMO1 levels attenuated miR-146a–mediated adverse cardiac remodeling and dysfunction (Figure 5E and 5F, Online Figure VB and Online Table VI). Finally, overexpression of miR-146a dramatically increased mortality in negative littermates mice; however, this miR-146a–mediated fatality was significantly attenuated in SUMO1 TG mice, as shown by Kaplan-Meier analysis (Figure 5G). Collectively, these observations suggest that the detrimental effects of miR-146a are mainly mediated through downregulation of SUMO1 in the heart.

Fibroblasts Secrete and Transfer miR-146a Into Cardiomyocytes via Extracellular Vehicles

To further elucidate the regulatory mechanisms of miR-146a during HF, we examined mature miR-146a and primary transcript (pri-mir-146a) levels in 2 different heart cell fractions (cardiomyocytes and nonmyocytes). An ≈2.7-fold upregulation of miR-146a was observed in cardiomyocytes isolated from failing hearts, compared with wild-type cardiomyocytes (Figure 6A). However, pri-mir-146a was upregulated exclusively in the nonmyocyte fraction of failing hearts (Figure 6B). These observations led us to hypothesize that miR-146a is produced in nonmyocyte cells and then delivered to the cardiomyocytes. Intriguingly, recent studies have shown that cardiomyocytes do not induce miR-146a expression by direct stimulation, but rather receive it from other cardiac cells via EVs.[25,26,29] To identify the miR-146a–expressing cell type in the heart, the expression of mature miR-146a and pri-mir-146a was analyzed in the 4 major cardiac cell types (cardiomyocytes, fibroblasts, endothelial cells, and leukocytes) isolated by fluorescence-activated cell sorting (Online Figure VIA through VID and Online Table VII). Although mature miR-146a levels were increased in failing cardiomyocytes, pri-mir-146a levels did not alter under failing conditions, consistent with previous findings (Figure 6A and 6B). In contrast, a significant elevation in pri-mir-146a levels was observed predominantly in the fibroblast and leukocyte fractions in HF (Figure 6C and 6D).
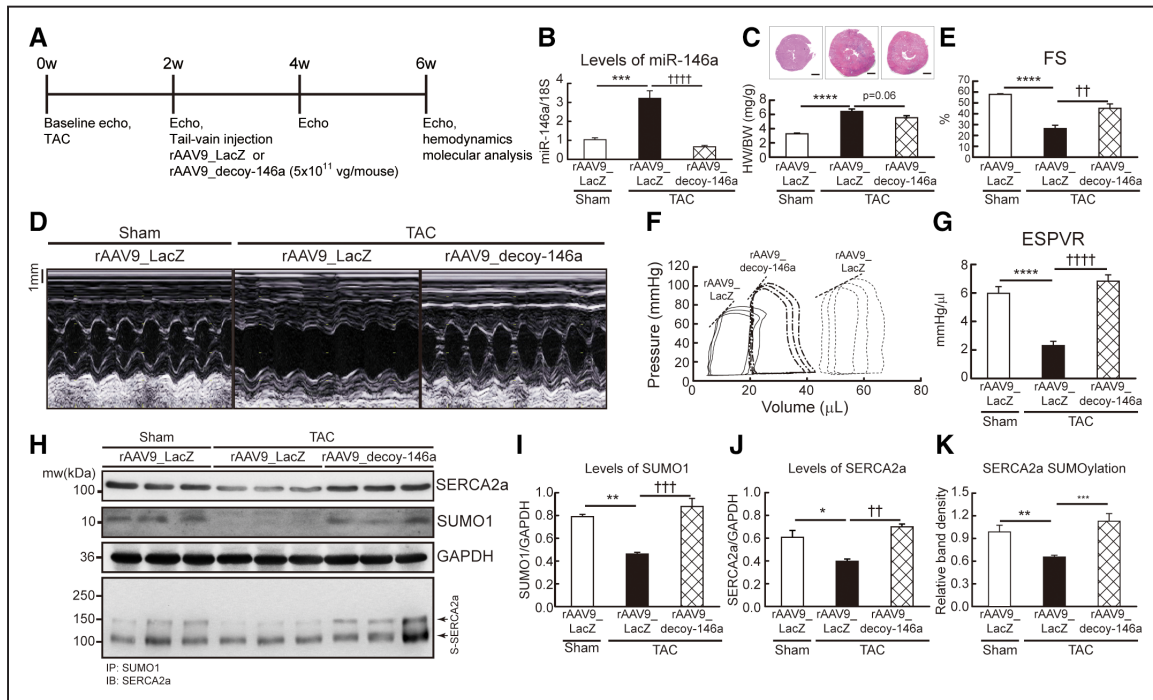
Figure 4. Inhibition of microRNA-146a (miR-146a) prevents cardiac dysfunction under pressure overload in vivo. A, Protocol for AAV9-decoy-146a gene transfer in mouse model of pressure overload. Six-week-old male B6C3/F1 mice were subjected to transverse aortic constriction (TAC) and received AAV9 carrying miR-146a decoy (rAAV9_decoy-146a, 5×10^{11} vg/mouse) or LacZ (beta-galactosidase; rAAV9_LacZ) via tail vein injection 2 wk post-TAC surgery. Cardiac function was measured by echocardiography and analyzed by hemodynamic measurements 4 wk after gene delivery. **B**, Levels of miR-146a. **C**, Cross-section images of a mouse heart (**top**) and quantification of heart weight/body weight ratio (**bottom**). Scale bars, 1 mm. **D, E**, Representative left ventricle (LV) M-mode images (**D**) and factional shortening (FS) (**E**) (n=8–10). **F, G**, Representative pressure-volume loops (**F**) and end-systolic pressure-volume relationship (ESPVR; **G**) (n=6–8). **H**, Representative blot showing SERCA2a (sarcoplasmic reticulum Ca^{2+}-ATPase), SUMO1 (small ubiquitin-like modifier 1), and total SUMOylation after infection of rAAV9_decoy-146a. **I–K**, Protein quantification of SUMO1 (**I**), SERCA2a (**J**), and SERCA2a SUMOylation (**K**) (n=6). *$P<0.05$, **$P<0.01$, ***$P<0.001$ vs sham-operated mice and ††$P<0.01$, †††$P<0.001$ vs the TAC-operated mice infected with rAAV9_LacZ, as determined by 1-way ANOVA. Data are represented as mean±SEM.

To compare the level of miR-146a secretion in fibroblasts and leukocytes, EVs were isolated from fibroblast and leukocyte cultures and then analyzed for miR-146a expression. The level of secreted miR-146a was ≈4-fold higher in EVs secreted from fibroblasts than from leukocytes (Figure 6E). Combined with the fact that fibroblasts are >14-fold more abundant than leukocytes in the heart (Online Table VII), this observation suggests that fibroblasts are the major source of secreted miR-146a in the heart. During HF, fibroblasts transdifferentiate into myofibroblasts, which induces dynamic changes in functional properties and gene expression.[30,31] To mimic pathogenic conditions, fibroblast cultures were treated with TGF-β (transforming growth factor-β), which is known as the primary factor that drives transdifferentiation of fibroblasts.[32,33] miR-146a expression was significantly increased after TGF-β treatment, paralleling the increase in transdifferentiation markers (Online Figure IVE and IVF). TGF-β treatment also enhanced EV-mediated miR-146a secretion by ≈20-fold, suggesting that TGF-β triggers the release of miR-146a from fibroblasts (Figure 6F). To confirm the uptake of released miR-146a into cardiomyocytes, EVs isolated from fibroblast cultures (Fib-EV) were labeled with a fluorescent dye (PKH-26) and added to isolated cardiomyocytes. Confocal microscopy revealed the presence of Fib-EVs in cardiomyocytes (Figure 6G and Online Figure VII). qRT-PCR analysis further confirmed that mature miR-146a levels, but not pri-mir-146a levels, increased in

cardiomyocytes after Fib-EV treatment. These results imply that the transfer of miR-146a via EVs is the main mechanism by which levels of miR-146a increase in cardiomyocytes and also excludes the possibility of EV treatment in promoting miR-146a synthesis (Figure 6H). The increase of miR-146a levels in cardiomyocytes was accompanied by a decrease in SUMO1 levels and reduced Ca^{2+} transient amplitude and cardiac contractility (Figure 6I and 6J and Online Table VIII). These findings indicate that transdifferentiation of fibroblasts, and hence miR-146a secretion, is the causative mechanism of miR-146a upregulation in cardiomyocytes during HF.

EV-Mediated miR-146a Transfer Is a Critical Mechanism of SUMO1 Regulation and Cardiac Function in Cardiomyocytes

To further confirm the role of EV-associated miR-146a on cardiomyocyte function, we examined the effect of either miR-146a–enriched or miR-146a–depleted EVs on cardiomyocyte function. We generated Fib-EVs in which miR-146a was either enriched (miR-146a–enriched EV) or depleted (miR-146a–depleted EV) by infection with either Ad_pre-mir-146a or Ad_decoy-146a, respectively. The effect of these EVs on cardiomyocyte function was then examined (Figure 7A and Online Figure VIIIA). miR-146a–enriched EVs contained an ≈2-fold higher level of miR-146a, whereas miR-146a–depleted EVs contained ≈20% of the miR-146a level in wild-type
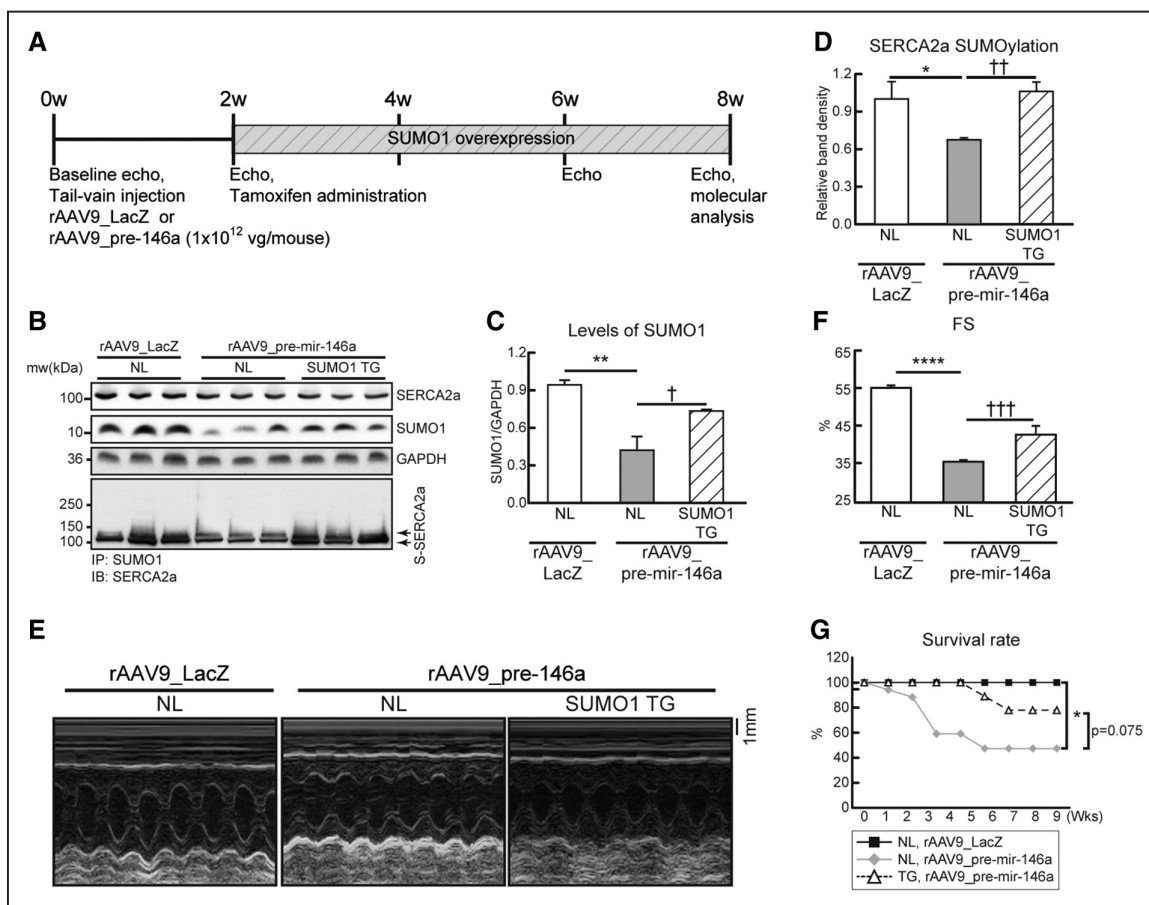
Figure 5. Complementation of SUMO1 (small ubiquitin-like modifier 1) expression attenuates microRNA-146a (miR-146a)–induced cardiac dysfunction in vivo. A, Protocol for SUMO1 reexpression in mouse model injected with rAAV9_pre-mir-146a. Six-week-old male B6C3/F1 mice were received AAV9 (adeno-associated virus serotype 9) carrying pre-miR-146a (rAAV9_pre-mir-146a, 1×10^{12} vg per mouse) or LacZ (beta-galactosidase; rAAV9_LacZ) via tail vein injection. Tamoxifen was administered to induce SUMO1 expression in the SUMO1 transgenic (TG) mice at 2 wk post-rAAV9_pre-mir-146a injection. Cardiac function was measured by echocardiography and analyzed by hemodynamic measurements 8 wk after gene delivery. **B**, Representative blot showing SERCA2a (sarcoplasmic reticulum Ca^{2+}-ATPase), SUMO1, and total SUMOylation after infection of rAAV9_decoy-146a. **C**, **D**, The protein quantification of SUMO1 (**C**) and SERCA2a SUMOylation (**D**) protein levels (n=6). **E**, **F**, Representative left ventricle (LV) M-mode images (**E**) and factional shortening (FS) (**F**) (n=5–8). **G**, Survival of animals after rAAV9_pre-mir-146a in negative littermate (NL) or SUMO1 TG. The Kaplan-Meier method was used to analyze animal lifespan (NL with rAAV9_LacZ, n=10; NL with rAAV9_pre-mir-146a, n=17; TG with rAAV9_pre-mir-146a, n=9). *P<0.05, **P<0.01, ***P<0.001 vs NL mice injected with rAAV9_LacZ and ††P<0.01, †††P<0.001 vs NL mice injected with rAAV9_pre-mir-146a, as determined by 1-way ANOVA. Data are represented as mean±SEM.

Fib-EVs (Figure 7B). Cardiomyocytes treated with miR-146a–enriched EVs exhibited increased miR-146a levels, decreased SUMO1 levels, and impaired Ca^{2+} transients and contractility, whereas cardiomyocytes treated with miR-146a–depleted EVs exhibited slightly decreased miR-146a levels, increased SUMO1 levels, and improved Ca^{2+} transients and contractility, compared with cells treated with wild-type Fib-EVs (Figure 7C through 7E and Online Table VIII).

In addition, to clarify the pivotal role of miR-146a in EV delivery in cardiomyocyte functions, the effects of miR-146a inhibition against Fib-EVs were tested. The isolated cardiomyocytes were pretreated with Ad_decoy-146a and then treated with Fib-EV for 24 hours after which calcium transient and cardiomyocyte contractility were measured (Online Figure VIIIB). As expected, Ad_decoy-146a pretreatment blocked the negative inotropic effects that were brought up by upregulation of miR-146a because of Fib-EV uptake (Online Figure VIIIC through VIIIE).

Finally, to address the physiological relevance of EV-mediated miR-146a transfer in vivo, isolated cardiomyocytes

were treated with EVs isolated from wild-type (Sham-EV) or failing mouse hearts (HF-EV) (Figure 7F and Online Figure VIIIF). The level of miR-146a in EVs isolated from failing hearts was ≈6-fold higher than in the wild-type control (Figure 7G, Online Figure VIIIG and VIIIH). Treatment of wild-type cardiomyocytes with EVs isolated from failing hearts resulted in increased miR-146a levels and decreased SUMO1 expression and significantly impaired Ca^{2+} transients and cardiac contractility, compared with cardiomyocytes treated with EVs isolated from wild-type hearts (Figure 7H through 7J and Online Table VIII). Collectively, these data suggest that EV-mediated delivery of miR-146a to cardiomyocytes plays a pivotal role in SUMO1 regulation during HF.

Discussion

To the best of our knowledge, this study is the first to demonstrate that the upregulation of miR-146a has a direct correlation with the reduction of SUMO1 levels in failing hearts. The reduction of SUMO1 expression by miR-146a overexpression resulted in decreased SERCA2a SUMOylation and contractile
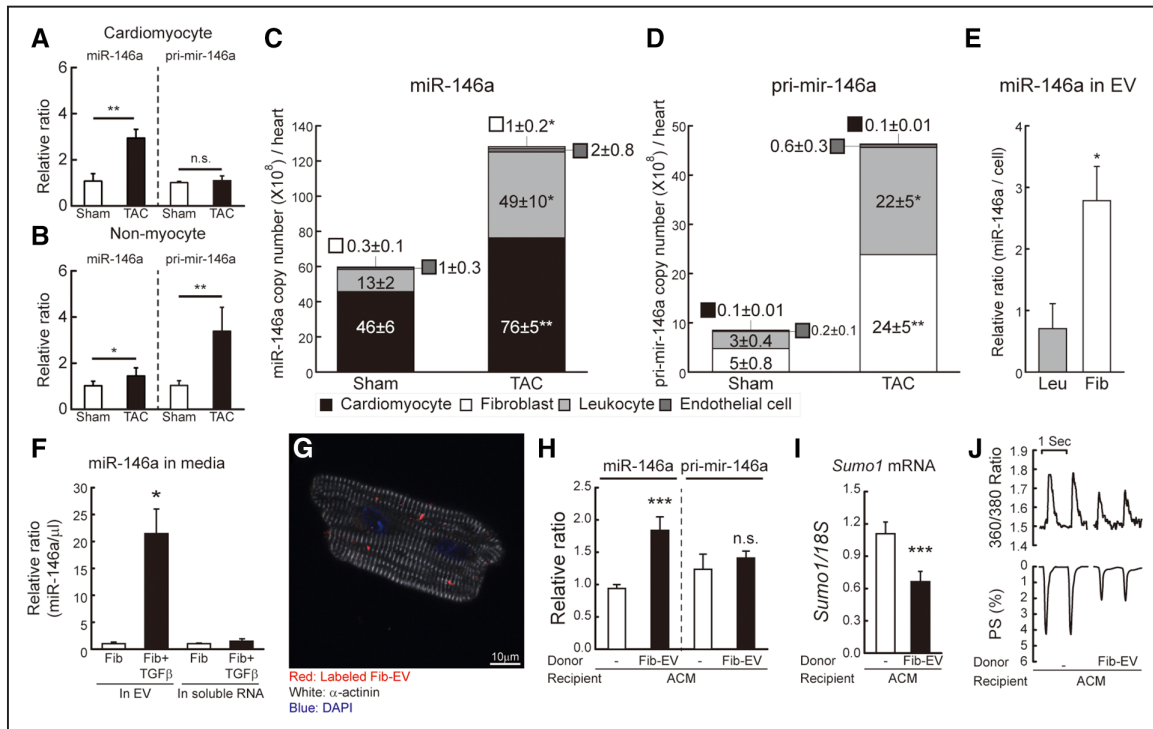
Figure 6. miR-146a is transferred from fibroblasts into cardiomyocytes through an extracellular vesicle (EV)–mediated mechanism. A, **B**, Changes in miR-146a and pri-mir-146a levels in isolated cardiomyocyte (**A**) or nonmyocyte (**B**) fractions from mouse hearts of sham-operated and transverse aortic constriction (TAC)–operated mice (6 wk after TAC) (n=3). The RNA levels were normalized to 18S rRNA. **C**, **D**, Copy number of miR-146a (**C**) and pri-mir-146a (**D**) in sorted cardiac cells from sham- and TAC-operated mice (6 wk after TAC) (n=5). **E**, Levels of miR-146a in isolated EVs from leukocyte (Leu) or fibroblast (Fib)-cultured media. **F**, Levels of miR-146a in isolated EVs from fibroblast-cultured media with/without TGF-β (transforming growth factor-β. **G**, Representative confocal microscopic image of isolated cardiomyocytes treated with labeled EVs for 24 h. **H**, **I**, Levels of miR-146a, pri-mir-146a (**H**) and SUMO1 mRNA (**I**) in isolated cardiomyocytes treated with/without fibroblast-derived EVs for 24 h (n=3). **J**, Representative trace of calcium transient (**top**) and cardiac contractility (**bottom**) (n=60–80 cells per 3 hearts). *P<0.05, **P<0.01, ***P<0.001 vs the indicated control, as determined by Student t test. Data are represented as mean±SEM.

function in cardiomyocytes. Moreover, inhibition of miR-146a reversed contractile dysfunction in failing hearts by restoring SUMO1 levels. In failing hearts, miR-146a was secreted from transdifferentiated fibroblasts and then transferred into cardiomyocytes by EV-mediated trafficking. This intracellular communication promoted the inhibition of SUMO1 expression in cardiomyocytes, resulting in cardiac dysfunction during HF. A schematic summary of our findings is shown in Figure 8.

SUMOylation is a post-translational modification process in which SUMO proteins are conjugated to their targets via enzymatic cascade reactions.[34] This process has been shown to regulate proteins by altering their structure, enzymatic activity, stability, subcellular localization, and protein-protein interactions.[34] Recent studies have demonstrated that the SUMO pathway is central in regulating heart development, with defective SUMOylation leading to congenital heart defects.[35] Global SUMO1-knockout mice develop congenital heart disease, including atrial and ventricular septal defects, and cardiac-specific SUMO1-knockdown mice show a progression of cardiac dysfunction and sudden death.[35] The absence of SENP2 (sentrin-specific protease 2), a deSUMOylating enzyme, leads to embryonic lethality with defects in the embryonic mouse heart.[36] In addition, cardiac-specific SENP2 overexpression mice exert dilated cardiomyopathy, further underlining the importance of maintaining proper SUMOylation in the heart.[37] Our group has previously

shown that SERCA2a SUMOylation occurring at lysine 480 and lysine 585 is essential for correct SERCA2a ATPase activity and protein stability in human and mouse cells.[10] SUMO1 and SUMOylated SERCA2a levels are reduced in failing human and mouse hearts. However, AAV-mediated SUMO1 gene transfer has exhibited significant beneficial effects in HF animal models.[10–12] Recently, our group showed that the small molecule N106 directly activates the SUMO-activating enzyme, SUMO E1 ligase, and induces intrinsic SERCA2a SUMOylation.[38] Previous studies have demonstrated that N106 improves ventricular function in HF mice models, suggesting that SUMO1 targeting could serve as the basis for the design of new therapies for countering HF.

In this study, we set out to identify miRs that target and regulate SUMO1 expression in HF. We identified miR-146a as a potential SUMO1-targeting miR using in silico prediction tools. Indeed, miR-146a directly binds a site ≈20 to 50 bp downstream of the 3′-UTR of the *Sumo1* gene, as determined by our luciferase assay. miR-146a overexpression significantly reduced a monomeric form of SUMO1 and SUMO1 conjugates in vitro and in vivo. The reduction in global SUMOylation significantly decreased SUMOylation of SERCA2a. In contrast, miR-146a inhibition attenuated SUMO1 reductions and restored SERCA2a SUMOylation. We also tested other SUMOylation targets in the same experimental condition, but these proteins (Sp1, GATA4)
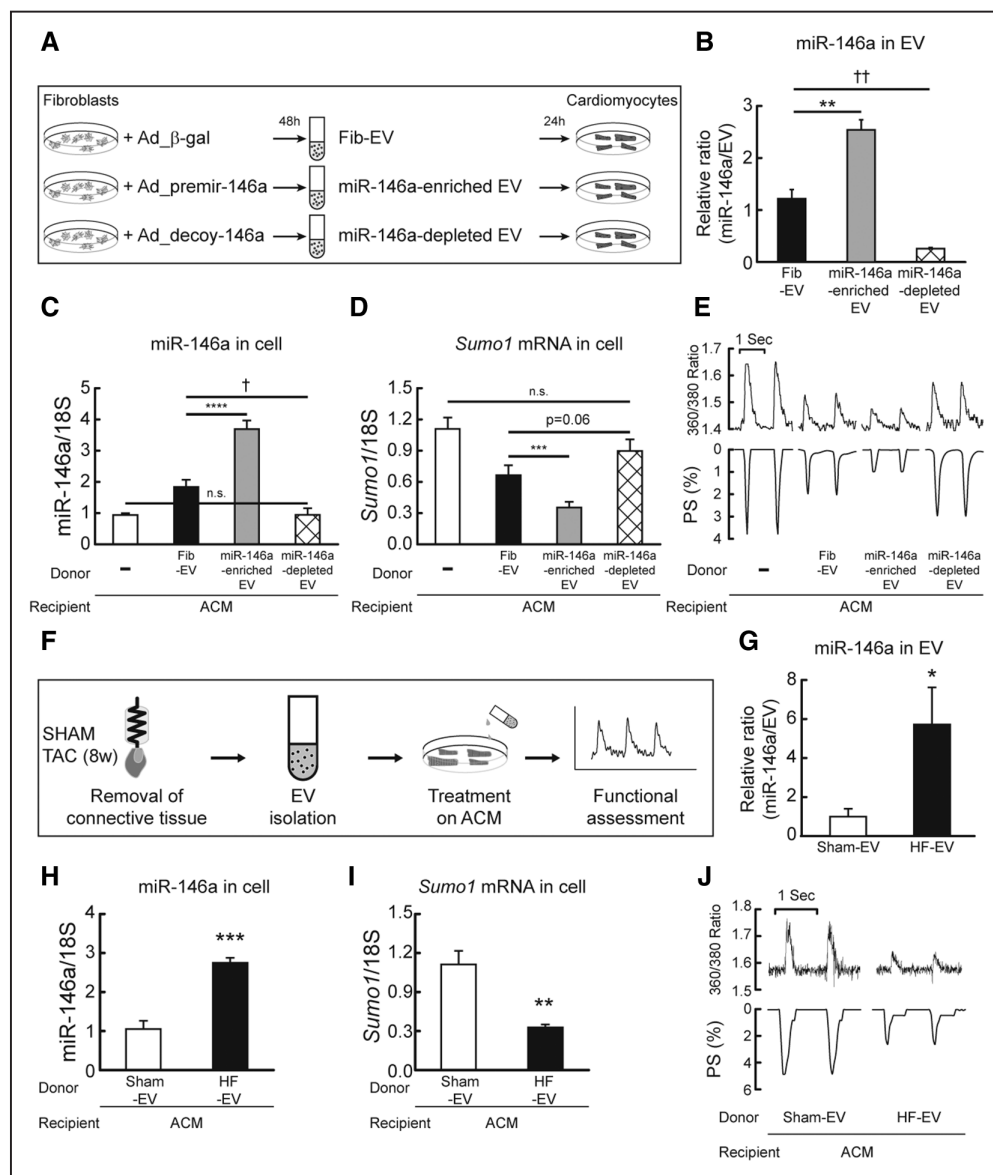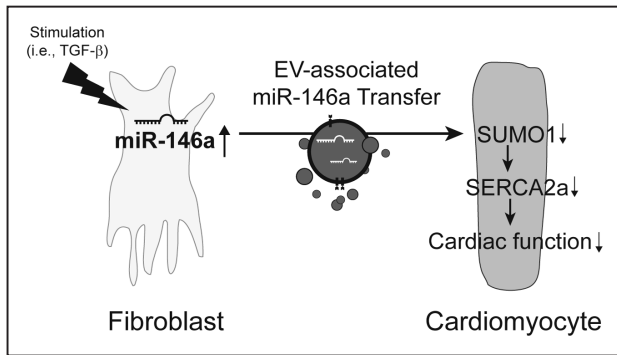
Figure 7. Extracellular vesicle (EV)–mediated miR-146a transfer affects cardiac function. A, Scheme depicting a protocol used for the production of miR-146a–enriched or miR-146a–depleted EVs. **B**, Levels of miR-146a in fibroblast-derived (EVs isolated from fibroblast cultures [Fib–EV]), miR-146a–enriched fibroblast-derived (miR-146a–enriched EV), and miR-146a–depleted fibroblast-derived (miR-146a depleted EV) EVs. **C, D**, Levels of miR-146a (**C**) and SUMO1 (small ubiquitin-like modifier 1) mRNA (**D**) in isolated adult cardiomyocytes (ACMs) nontreated or treated with Fib-EV, miR-146a–enriched EV, or miR-146a–depleted EV for 24 h (n=4). **E**, Representative trace of calcium transients (**top**) and cardiac contractility (**bottom**) (n=60–80 cells per 3 hearts). **F**, Scheme depicting a protocol used for the isolation of EVs from normal and failing hearts. **G**, Levels of miR-146a in EVs from normal (Sham-EV) and failing mouse hearts (heart failure [HF]-EV) (6 wk after transverse aortic constriction [TAC], n=3). **H, I**, Levels of miR-146a (**H**) and SUMO1 mRNA (**I**) in isolated cardiomyocytes treated with Sham-EVs or HF-EVs for 24 h (n=3). **J**, Representative trace of calcium transient (**top**) and cardiac contractility (**bottom**) (n=60–80 cells per 3 hearts). *$P<0.05$, **$P<0.01$, ***$P<0.001$, †$P<0.05$, ††$P<0.01$ vs the indicated control, as determined by Student t test. Data are represented as mean±SEM. PS indicates peak shortening.

were not susceptible to the changes of SUMO1 expression as much as SERCA2a (Online Figure IIIJ and IVH). The features of SERCA2a SUMOylation, that is, SUMOylated only by the SUMO1 isoform and does not require a specific SUMO E3 enzyme, seem to determine the susceptibility of SERCA2a SUMOylation to the levels of SUMO1 expression. The miR-146a–mediated reduction in SERCA2a SUMOylation certainly affected cardiac function and sudden death in mice, which is consistent with our previous findings about SUMO1 reduction in the heart.[10] In contrast, miR-146a inhibition preserved adverse remodeling and

dysfunction in TAC mice. Therefore, our findings may provide another attractive therapeutic target for the intervention of HF.

miR-146a was originally discovered as an innate immune suppressor in the THP-1 human monocytic cell line in which it targets IRAK1 and TRAF6.[17] Recent studies have reported that overexpression of miR-146a reduced the immune response in myocardial ischemia/reperfusion injury,[21] septic cardiomyopathy,[22] diabetic cardiomyopathy,[23] and myocardial infarction.[39] Another study using a human cardiac cell line (AC16) showed that miR-146a inhibition enhanced the

Figure 8. Schematic model depicting miR-146a regulation of SUMOylation in heart failure. During heart failure, miR-146a is expressed and processed in fibroblasts. The mature miR-146a is secreted as an extracellular vesicle (EV)–associated form from the activated fibroblasts and then transferred into cardiomyocytes. The fibroblast-derived miR-146a targets SUMO1 (small ubiquitin-like modifier 1) and attenuates SERCA2a (sarcoplasmic reticulum Ca^{2+}-ATPase) SUMOylation, thus reducing cardiomyocyte function. TGF-β indicates transforming growth factor-β.

expression of mRNAs related to inflammation.[40] Therefore, we were concerned about the excessive inflammation caused by miR-146a inhibition in the present study. To test whether miR-146a inhibition affects cardiac inflammation under pressure overload, representative inflammatory markers were quantified by qRT-PCR and immunohistochemistry. On the basis of our qRT-PCR results, although miR-146a levels were elevated, pressure overload stimulated the expression of inflammatory markers such as TNF (tumor necrosis factor)-α, CD11c, CD19, CD3, and F4/80 (Online Figure IXA through IXE). However, rAAV9_decoy-146a–mediated inhibition of miR-146a in failing hearts abolished inflammatory responses (Online Figure IXA through IXE). In addition, immunohistochemistry revealed that CD45 and TNF-α expression were significantly increased in failing hearts but decreased in decoy-146a–treated failing hearts (Online Figure IXF through IXH). These results imply that pressure overload drives the heart to induce inflammatory responses, regardless of the increase in miR-146a levels. In contrast, normalization of miR-146a levels exerted protective effects against inflammation under pressure overload. Thus, although previous reports have provided important evidence that miR-146a attenuates inflammatory response by suppressing its targets, under our HF model settings, we did not observe excessive inflammation and miR-146a inhibition showed beneficial effects on inflammatory responses. Further studies aimed at elucidating the reciprocal relationship between miR-146a and cardiac inflammation are currently underway.

Currently, 2 conflicting views exist on the role of miR-146a in the heart: beneficial versus deleterious effects. The supporting argument for the positive effect of miR-146a in the heart is based on evidence that miR-146a can act as an innate immune suppressor. On the contrary, reports have also shown that miR-146a suppresses the expression of critical proteins (DLST [dihydrolipoyl succinyltransferase], ERBB4 [Erb-B2 receptor tyrosine kinase 4], and NRAS [neuroblastoma RAS viral oncogene homolog]), which have been shown to play crucial roles in cardiac metabolism or angiogenesis.[24–26,41] These studies have demonstrated that inhibition of miR-146a

results in reduced cardiac damage in doxorubicin-induced, pressure overload, and peripartum cardiomyopathy animal models.[24–26] In agreement with these reports, our current study also shows beneficial effects of miR-146a inhibition on cardiac function. Taken together, the effects of miR-146a could vary on different physiological settings of disease. One potential possibility to explain the contradictory results related to miR-146a is the binary effect of an immune response in disease states. Immunologists think that the relative balance between pathological inflammatory pathways and tissue reparative processes defines the trajectory of HF development.[42] Suppression of immune response could be beneficial in disease models where pathological inflammation is strongly activated. However, if physiological inflammation is activated in tissue reparative processes, immune suppression is not the correct approach to protect the heart from damage. The role of miR-146a could differ depending on the involvement of pathological immune response. Therefore, the effects of miR-146a on cardiac function need further exploration in different settings of disease and caution needs to be taken when moving this study into clinical trials.

EVs are heterogeneously sized (20–2000 nm) particles released into biological fluids including blood, urine, tears, and pericardial fluid, as well as into conditioned media from cultured cells.[43,44] Recently, EVs have emerged as biological carriers, transferring their protein, lipid, mRNA, long noncoding RNA, and microRNA content to target cells.[43,44] In the heart, EVs are known to play important roles in intercellular communication between cardiac cells. Bang et al[45] suggested that cardiac fibroblast–derived EVs mediate cardiac hypertrophy through the prohypertrophic microRNA, miR-21*, and Wang et al[46] showed that diabetic cardiomyocyte–derived EVs reduce angiogenesis by transferring antiangiogenic miR-320 into endothelial cells. Recent studies have shown that miR-146a is also secreted in an EV-associated form.[25,26,29] miR-146a in endothelial cell–derived EVs exerts negative effects on cardiac function in peripartum cardiomyopathy and pressure overload models.[25,26] Intriguingly, these studies found that endothelial cell–derived EVs play a primary role in regulating miR-146a levels in cardiomyocytes. Because these previous studies used a single-cell culture model, we examined the overall changes in miR-146a expression in 4 major cardiac cell types during HF. According to our fluorescence-activated cell sorting analysis, cardiac fibroblasts produced the majority of miR-146a (Figure 6C and 6D). Consistent with previous studies, endothelial cells also exhibited upregulated expression of miR-146a in failing hearts; however, the level of miR-146a production was much lower than in fibroblasts (Figure 6C and 6D). Globally, however, fibroblasts seem to be the predominant source of miR-146a in the heart during HF. Another compelling finding was that the ratio between the number of EVs and cells was maintained at 2000:1 (EVs:cells) during HF, although the total number of EVs was doubled, as determined by nanoparticle tracking analysis (Online Figure VIIIF through VIIIH). We defined this ratio as physiologically relevant and tested the functional consequences of different EV/cell ratios. Therefore, our finding may serve as a standard ratio of the effects of EVs on cardiac cells in future studies.

In this study, we demonstrate a novel regulatory mechanism of cardiac function whereby cardiac fibroblasts influence cardiac contractility by diminishing the expression of SUMO1 via EV-associated delivery of miR-146a. In addition, the beneficial effects of miR-146a inhibition via decoy-146a on cardiac function suggest that targeting miR-146a may provide a novel therapeutic strategy for the treatment of HF.

Disclosures

None.

References

1. Marks AR. Calcium cycling proteins and heart failure: mechanisms and therapeutics. *J Clin Invest*. 2012;123:46–52.
2. Luo M, Anderson ME. Mechanisms of altered Ca²⁺ handling in heart failure. *Circ Res*. 2013;113:690–708. doi: 10.1161/CIRCRESAHA.113.301651
3. Mozaffarian D, Benjamin EJ, Go AS, et al; Writing Group Members; American Heart Association Statistics Committee; Stroke Stratistics Subcommittee. Heart disease and stroke statistics-2016 update: a report from the American Heart Association. *Circulation*. 2016;133:e38–e360. doi: 10.1161/CIR.0000000000000350
4. Miyamoto MI, del Monte F, Schmidt U, DiSalvo TS, Kang ZB, Matsui T, Guerrero JL, Gwathmey JK, Rosenzweig A, Hajjar RJ. Adenoviral gene transfer of SERCA2a improves left-ventricular function in aortic-banded rats in transition to heart failure. *Proc Natl Acad Sci USA*. 2000;97:793–798.
5. del Monte F, Hajjar RJ, Harding SE. Overwhelming evidence of the beneficial effects of SERCA gene transfer in heart failure. *Circ Res*. 2001;88:E66–E67.
6. Sakata S, Lebeche D, Sakata Y, Sakata N, Chemaly ER, Liang L, Nakajima-Takenaka C, Tsuji T, Konishi N, del Monte F, Hajjar RJ, Takaki M. Transcoronary gene transfer of SERCA2a increases coronary blood flow and decreases cardiomyocyte size in a type 2 diabetic rat model. *Am J Physiol Heart Circ Physiol*. 2007;292:H1204–H1207. doi: 10.1152/ajpheart.00892.2006
7. Kawase Y, Ly HQ, Prunier F, et al. Reversal of cardiac dysfunction after long-term expression of SERCA2a by gene transfer in a pre-clinical model of heart failure. *J Am Coll Cardiol*. 2008;51:1112–1119.
8. Jaski BE, Jessup ML, Mancini DM, Cappola TP, Pauly DF, Greenberg B, Borow K, Dittrich H, Zsebo KM, Hajjar RJ; Calcium Up-Regulation by Percutaneous Administration of Gene Therapy In Cardiac Disease (CUPID) Trial Investigators. Calcium upregulation by percutaneous administration of gene therapy in cardiac disease (CUPID Trial), a first-in-human phase ½ clinical trial. *J Card Fail*. 2009;15:171–181. doi: 10.1016/j.cardfail.2009.01.013
9. Jessup M, Greenberg B, Mancini D, Cappola T, Pauly DF, Jaski B, Yaroshinsky A, Zsebo KM, Dittrich H, Hajjar RJ; Calcium Upregulation by Percutaneous Administration of Gene Therapy in Cardiac Disease (CUPID) Investigators. Calcium Upregulation by Percutaneous Administration of Gene Therapy in Cardiac Disease (CUPID): a phase 2 trial of intracoronary gene therapy of sarcoplasmic reticulum Ca2+-ATPase in patients with advanced heart failure. *Circulation*. 2011;124:304–313. doi: 10.1161/CIRCULATIONAHA.111.022889
10. Kho C, Lee A, Jeong D, Oh JG, Chaanine AH, Kizana E, Park WJ, Hajjar RJ. SUMO1-dependent modulation of SERCA2a in heart failure. *Nature*. 2011;477:601–605. doi: 10.1038/nature10407
11. Tilemann L, Lee A, Ishikawa K, Aguero J, Rapti K, Santos-Gallego C, Kohlbrenner E, Fish KM, Kho C, Hajjar RJ. SUMO-1 gene transfer improves cardiac function in a large-animal model of heart failure. *Sci Transl Med*. 2013;5:211ra159.
12. Lee A, Jeong D, Mitsuyama S, Oh JG, Liang L, Ikeda Y, Sadoshima J, Hajjar RJ, Kho C. The role of SUMO-1 in cardiac oxidative stress and hypertrophy. *Antioxid Redox Signal*. 2014;21:1986–2001. doi: 10.1089/ars.2014.5983
13. Bartel DP. MicroRNAs: target recognition and regulatory functions. *Cell*. 2009;136:215–233. doi: 10.1016/j.cell.2009.01.002
14. Melman YF, Shah R, Das S. MicroRNAs in heart failure: is the picture becoming less miRky? *Circ Heart Fail*. 2014;7:203–214. doi: 10.1161/CIRCHEARTFAILURE.113.000266
15. van Rooij E, Marshall WS, Olson EN. Toward microRNA-based therapeutics for heart disease: the sense in antisense. *Circ Res*. 2008;103:919–928. doi: 10.1161/CIRCRESAHA.108.183426
16. Wahlquist C, Jeong D, Rojas-Muñoz A, Kho C, Lee A, Mitsuyama S, van Mil A, Park WJ, Sluijter JP, Doevendans PA, Hajjar RJ, Mercola M. Inhibition of miR-25 improves cardiac contractility in the failing heart. *Nature*. 2014;508:531–535. doi: 10.1038/nature13073
17. Taganov KD, Boldin MP, Chang KJ, Baltimore D. NF-kappaB-dependent induction of microRNA miR-146, an inhibitor targeted to signaling proteins of innate immune responses. *Proc Natl Acad Sci USA*. 2006;103:12481–12486. doi: 10.1073/pnas.0605298103
18. Guo M, Mao X, Ji Q, Lang M, Li S, Peng Y, Zhou W, Xiong B, Zeng Q. miR-146a in PBMCs modulates Th1 function in patients with acute coronary syndrome. *Immunol Cell Biol*. 2010;88:555–564. doi: 10.1038/icb.2010.16
19. Pauley KM, Stewart CM, Gauna AE, Dupre LC, Kuklani R, Chan AL, Pauley BA, Reeves WH, Chan EK, Cha S. Altered miR-146a expression in Sjögren's syndrome and its functional role in innate immunity. *Eur J Immunol*. 2011;41:2029–2039. doi: 10.1002/eji.201040757
20. Xu WD, Lu MM, Pan HF, Ye DQ. Association of microRNA-146a with autoimmune diseases. *Inflammation*. 2012;35:1525–1529. doi: 10.1007/s10753-012-9467-0
21. Wang X, Ha T, Liu L, Zou J, Zhang X, Kalbfleisch J, Gao X, Williams D, Li C. Increased expression of microRNA-146a decreases myocardial ischaemia/reperfusion injury. *Cardiovasc Res*. 2013;97:432–442. doi: 10.1093/cvr/cvs356
22. Gao M, Wang X, Zhang X, Ha T, Ma H, Liu L, Kalbfleisch JH, Gao X, Kao RL, Williams DL, Li C. Attenuation of cardiac dysfunction in polymicrobial sepsis by microRNA-146a is mediated via targeting of IRAK1 and TRAF6 expression. *J Immunol*. 2015;195:672–682. doi: 10.4049/jimmunol.1403155
23. Feng B, Chen S, Gordon AD, Chakrabarti S. miR-146a mediates inflammatory changes and fibrosis in the heart in diabetes. *J Mol Cell Cardiol*. 2017;105:70–76. doi: 10.1016/j.yjmcc.2017.03.002
24. Horie T, Ono K, Nishi H, Nagao K, Kinoshita M, Watanabe S, Kuwabara Y, Nakashima Y, Takanabe-Mori R, Nishi E, Hasegawa K, Kita T, Kimura T. Acute doxorubicin cardiotoxicity is associated with miR-146a-induced inhibition of the neuregulin-ErbB pathway. *Cardiovasc Res*. 2010;87:656–664. doi: 10.1093/cvr/cvq148
25. Halkein J, Tabruyn SP, Ricke-Hoch M, Haghikia A, Nguyen NQ, Scherr M, Castermans K, Malvaux L, Lambert V, Thiry M, Sliwa K, Noel A, Martial JA, Hilfiker-Kleiner D, Struman I. MicroRNA-146a is a therapeutic target and biomarker for peripartum cardiomyopathy. *J Clin Invest*. 2013;123:2143–2154. doi: 10.1172/JCI64365
26. Heggermont WA, Papageorgiou AP, Quaegebeur A, et al. Inhibition of microRNA-146a and overexpression of its target dihydrolipoyl succinyltransferase protect against pressure overload-induced cardiac hypertrophy and dysfunction. *Circulation*. 2017;136:747–761. doi: 10.1161/CIRCULATIONAHA.116.024171
27. Paterson MR, Kriegel AJ. MiR-146a/b: a family with shared seeds and different roots. *Physiol Genomics*. 2017;49:243–252. doi: 10.1152/physiolgenomics.00133.2016
28. Mullokandov G, Baccarini A, Ruzo A, Jayaprakash AD, Tung N, Israelow B, Evans MJ, Sachidanandam R, Brown BD. High-throughput assessment of microRNA activity and function using microRNA sensor and decoy libraries. *Nat Methods*. 2012;9:840–846. doi: 10.1038/nmeth.2078
29. Alexander M, Hu R, Runtsch MC, Kagele DA, Mosbruger TL, Tolmachova T, Seabra MC, Round JL, Ward DM, O'Connell RM. Exosome-delivered microRNAs modulate the inflammatory response to endotoxin. *Nat Commun*. 2015;6:7321. doi: 10.1038/ncomms8321
30. Travers JG, Kamal FA, Robbins J, Yutzey KE, Blaxall BC. Cardiac fibrosis: the fibroblast awakens. *Circ Res*. 2016;118:1021–1040. doi: 10.1161/CIRCRESAHA.115.306565
31. Gyöngyösi M, Winkler J, Ramos I, Do QT, Firat H, McDonald K, González A, Thum T, Díez J, Jaisser F, Pizard A, Zannad F. Myocardial fibrosis: biomedical research from bench to bedside. *Eur J Heart Fail*. 2017;19:177–191. doi: 10.1002/ejhf.696

32. Dobaczewski M, Chen W, Frangogiannis NG. Transforming growth factor (TGF)-β signaling in cardiac remodeling. *J Mol Cell Cardiol.* 2011;51:600–606. doi: 10.1016/j.yjmcc.2010.10.033

33. Stempien-Otero A, Kim DH, Davis J. Molecular networks underlying myofibroblast fate and fibrosis. *J Mol Cell Cardiol.* 2016;97:153–161. doi: 10.1016/j.yjmcc.2016.05.002

34. Geiss-Friedlander R, Melchior F. Concepts in sumoylation: a decade on. *Nat Rev Mol Cell Biol.* 2007;8:947–956. doi: 10.1038/nrm2293

35. Wang J, Chen L, Wen S, Zhu H, Yu W, Moskowitz IP, Shaw GM, Finnell RH, Schwartz RJ. Defective sumoylation pathway directs congenital heart disease. *Birth Defects Res A Clin Mol Teratol.* 2011;91:468–476. doi: 10.1002/bdra.20816

36. Kang X, Qi Y, Zuo Y, Wang Q, Zou Y, Schwartz RJ, Cheng J, Yeh ET. SUMO-specific protease 2 is essential for suppression of polycomb group protein-mediated gene silencing during embryonic development. *Mol Cell.* 2010;38:191–201. doi: 10.1016/j.molcel.2010.03.005

37. Kim EY, Chen L, Ma Y, Yu W, Chang J, Moskowitz IP, Wang J. Enhanced desumoylation in murine hearts by overexpressed SENP2 leads to congenital heart defects and cardiac dysfunction. *J Mol Cell Cardiol.* 2012;52:638–649. doi: 10.1016/j.yjmcc.2011.11.011

38. Kho C, Lee A, Jeong D, Oh JG, Gorski PA, Fish K, Sanchez R, DeVita RJ, Christensen G, Dahl R, Hajjar RJ. Small-molecule activation of SERCA2a SUMOylation for the treatment of heart failure. *Nat Commun.* 2015;6:7229. doi: 10.1038/ncomms8229

39. Huang W, Tian SS, Hang PZ, Sun C, Guo J, Du ZM. Combination of microRNA-21 and microRNA-146a attenuates cardiac dysfunction and apoptosis during acute myocardial infarction in mice. *Mol Ther Nucleic Acids.* 2015;5:e296.

40. Palomer X, Capdevila-Busquets E, Botteri G, Davidson MM, Rodríguez C, Martínez-González J, Vidal F, Barroso E, Chan TO, Feldman AM, Vázquez-Carrera M. miR-146a targets Fos expression in human cardiac cells. *Dis Model Mech.* 2015;8:1081–1091. doi: 10.1242/dmm.020768

41. Odiete O, Hill MF, Sawyer DB. Neuregulin in cardiovascular development and disease. *Circ Res.* 2012;111:1376–1385. doi: 10.1161/CIRCRESAHA.112.267286

42. Dick SA, Epelman S. Chronic heart failure and inflammation: what do we really know? *Circ Res.* 2016;119:159–176. doi: 10.1161/CIRCRESAHA.116.308030

43. Kosaka N, Yoshioka Y, Hagiwara K, Tominaga N, Katsuda T, Ochiya T. Trash or treasure: extracellular microRNAs and cell-to-cell communication. *Front Genet.* 2013;4:173. doi: 10.3389/fgene.2013.00173

44. Raposo G, Stoorvogel W. Extracellular vesicles: exosomes, microvesicles, and friends. *J Cell Biol.* 2013;200:373–383. doi: 10.1083/jcb.201211138

45. Bang C, Batkai S, Dangwal S, et al. Cardiac fibroblast-derived microRNA passenger strand-enriched exosomes mediate cardiomyocyte hypertrophy. *J Clin Invest.* 2014;124:2136–2146. doi: 10.1172/JCI70577

46. Wang X, Huang W, Liu G, Cai W, Millard RW, Wang Y, Chang J, Peng T, Fan GC. Cardiomyocytes mediate anti-angiogenesis in type 2 diabetic rats through the exosomal transfer of miR-320 into endothelial cells. *J Mol Cell Cardiol.* 2014;74:139–150. doi: 10.1016/j.yjmcc.2014.05.001